ELSEVIER

Journal of Alloys and Compounds 320 (2001) 140–148

Journal of ALLOYS AND COMPOUNDS

www.elsevier.com/locate/jallcom

The thermal behavior of amorphous rhodium hydrous oxide

A. Šarić[a,*], S. Popović[b], R. Trojko[a], S. Musić[a]

[a]*Division of Materials Chemistry, Ruđer Bošković Institute, P.O. Box 180, 10002 Zagreb, Croatia*
[b]*Department of Physics, Faculty of Science, University of Zagreb, P.O. Box 331, 10002 Zagreb, Croatia*

Received 11 December 2000; accepted 24 January 2001

Abstract

Amorphous rhodium hydrous oxide precursors, precipitated from an $Rh(NO_3)_3$ solution with the addition of NH_3, NaOH or urotropin, were thermally treated in the range 300–1000°C. The obtained amorphous rhodium hydrous oxide precursors and their thermal decomposition products were studied by X-ray powder diffraction, Fourier transform infrared spectroscopy, differential thermal analysis and thermogravimetric analysis. Generally, the thermal behavior of amorphous rhodium hydrous oxide precursors depended on several parameters, such as pH, aging time, temperature, type of atmosphere and the presence of urotropin or products of its chemical decomposition. The thermal behavior of the amorphous rhodium hydrous oxides obtained by the addition of NH_3·aq at pH~10.4 differed in air or argon atmosphere. Heating in an argon atmosphere led to the partial autoreduction of the rhodium metal. After the calcination of the starting material at 500°C, two crystalline phases, α-Rh_2O_3 and RhO_2, were obtained. With a further increase in the temperature, RhO_2 was reduced. α-Rh_2O_3 was present as a single phase at 650°C in air, whereas β-Rh_2O_3 was present as a single phase at 1000°C. Although all starting rhodium hydrous oxide precursors obtained by the abrupt addition of an NaOH solution at pH~9 were amorphous, the phase composition of their thermal decomposition products varied depending on the time of the hydrothermal reaction. The crystallization products at 400°C, produced from amorphous rhodium hydrous oxides aged at 90°C between 3 and 21 days were amorphous, whereas the precursor aged for 1 day at 90°C yielded α-Rh_2O_3 and RhO_2 at 400°C. At higher temperatures, RhO_2 decomposed irreversibly to α-Rh_2O_3, which was the single phase at 500 and 600°C. After calcination at 900°C, β-Rh_2O_3 additionally crystallized to α-Rh_2O_3. The appearance of crystalline oxide phases was shifted to higher temperatures with an increase in the time of the hydrothermal reaction at 90°C. During the thermal treatment of amorphous rhodium hydrous oxide prepared in the presence of urotropin, the explosion effect was observed. The formation of nanocrystalline rhodium metal was observed at 300°C after heating amorphous rhodium hydrous oxide precipitated for 1 day in the presence of urotropine. The crystallite size of the thus produced rhodium was 6(2) nm. After additional thermal treatment at up to 825°C, a mixture of β-Rh_2O_3 and α-Rh_2O_3 was obtained.

Keywords: Rhodium hydrous oxide; α-Rh_2O_3; β-Rh_2O_3; RhO_2; Rh; X-ray diffraction; FT-IR; DTA; TGA

1. Introduction

Rhodium undergoes various redox reactions during its application in catalysis. In many cases, the role of rhodium in catalytic reactions is closely related to the formation of rhodium oxides (group name). Knowledge of the formation of rhodium oxides and the corresponding redox reactions is important for understanding the nature of catalytic processes. However, in the literature there is a discrepancy between the number of publications on the catalytic effects of rhodium on various substrates and the changes in the chemical state of rhodium in catalytic reactions. Rhodium oxides can be produced by the thermal decomposition of $Rh(OH)_3$ or various rhodium salts.

Bayer and Wiedemann [1] investigated the thermal behavior of $Rh(OH)_3$, $Rh(NO_3)_3 \cdot 6H_2O$ and $Rh_2(SO_4)_3 \cdot xH_2O$. RhO_2 (rutile-type) was obtained by the thermal decomposition of $Rh(OH)_3$ and $Rh(NO_3)_3 \cdot 6H_2O$ at 450–600°C in air. With a further increase in temperature, the formation of α-Rh_2O_3 (corundum-type) and β-Rh_2O_3 (orthorhombic) was observed. In a reducing atmosphere (N_2–H_2) at about 100–150°C, α-Rh_2O_3 and β-Rh_2O_3 were reduced to Rh°. Moran-Miguelez and Alario-Franco [2] used hydrothermal synthesis for the preparation of RhOOH and RhO_2. The DTA of RhOOH in air showed three endothermic peaks at 470, 900 and 1080°C, corresponding to the formation of RhO_2, α-Rh_2O_3 and Rh°,

*Corresponding author.
E-mail address: asaric@rudjer.irb.hr (A. Šarić).

0925-8388/01/$ – see front matter
PII: S0925-8388(01)00938-0

respectively. It was also possible to produce RhOOH hydrothermally from RhO_2 in pure water at 600°C and 1500 bars. Rh_2O_3 was easily reduced by hydrogen at 150°C. Prosychev et al. [3] obtained $Rh(OH)_3 \cdot 2H_2O$ precipitate from an $RhCl_3$ solution in a strongly alkaline medium. $Rh(OH)_3 \cdot 2H_2O$ lost two water molecules at 119±3°C, whereas RhO_2 was obtained between 190 and 230°C. With a further increase in temperature, RhO_2 decomposed to Rh_2O_3 at between 635 and 670°C. Crimp and Spiccia [4] prepared monomer, dimer and trimer hydroxy complexes of Rh^{3+}, which were neutralized in the next step by imidazole to produce yellow $Rh(OH)_3$ precipitate. After heating this precipitate at 250 to 300°C in air, RhO_2 was obtained due to oxidation, $Rh^{3+} \rightarrow Rh^{4+}$. The end product of the thermal treatment of the $Rh(OH)_3$ precipitate, in air or nitrogen, was α-Rh_2O_3. The maximum heating temperature did not exceed 615°C.

Electrodes activated with platinum group oxides are important materials in electrocatalysis. Generally, these electrodes can be prepared by thermal treatment, usually of a Ti electrode previously dipped in an acidic solution of corresponding salts. Roginskaya et al. [5] thermally treated Ti electrodes previously dipped in an $RhCl_3$+HCl aqueous solution. The obtained film was amorphous up to 466°C. Following treatment at 500°C, broad and diffuse XRD lines of α-Rh_2O_3 appeared, whereas those of TiO_2, α-Rh_2O_3 and TiO_2 were present in the film obtained at 600°C. At lower temperatures in the film, chlorine was detected, and it was supposed that $RhO(OH)_{1-x}Cl_x$ was an active compound in the electrocatalytic processes. Rhodium oxides also show electrochromic properties [6]. Anodically oxidized rhodium electrodes showed color changes upon cycling the electric potential. The color changes varied between yellow and dark green for thin oxide films, whereas changes from yellow to brown purple were observed for thicker films. However, in the case of rhodium oxide electrochromism, the anodic peak, giving rise to coloration in the cyclic voltammogram, overlaps heavily with the onset of O_2 evolution. This means that full coloration could not be achieved without a simultaneous O_2 evolution occurring as a side-reaction. Jerkiewicz and Borodzinski [7] studied the relation between the surface state of rhodium oxide and the kinetics of the oxygen evolution reactions. The oxide film formed during anodic polarization consisted mainly of $Rh(OH)_3$ with a submonolayer film of RhO(OH). This very thin hydrous oxide film was in direct contact with the electrolyte and an oxygen evolution reaction takes place at this interface.

The aim of the present work was to correlate the preparation of amorphous rhodium hydrous oxide and its thermal behavior, since this problem has not received proper attention in previous works. The samples of amorphous rhodium hydrous oxide were prepared under highly controlled conditions using the 'wet' precipitation method. It is generally known from precipitation chemistry that the preparation of the metal hydrous oxide precursor influences the thermal behavior of this material and can even change the route of crystallization.

2. Experimental

Chemicals of analytical purity and doubly distilled water were used. The $Rh(NO_3)_3 \cdot 2H_2O$ salt was dissolved in doubly distilled water. Amorphous rhodium hydrous oxides were precipitated from an $Rh(NO_3)_3$ solution by the addition of an $NH_3 \cdot$aq. or NaOH solution with very intense mixing. Amorphous rhodium hydrous oxides were also precipitated in the presence of decomposing urotropin. The sample denoted as S1 was obtained using the following procedure. Into 200 ml of 0.2 M $Rh(NO_3)_3$ solution, 200 ml of doubly distilled water was added and then under intense mixing an amorphous rhodium hydrous oxide was precipitated by adding 50 ml of 25% $NH_3 \cdot$aq. After 1 h of ageing at room temperature, the precipitate was subsequently washed and then dried at 60°C for 48 h. The synthesis conditions for samples S2–S10 are given in Table 1. The precipitate was separated using an ultraspeed centrifuge, Sorvall RC2-B (operational range up to 20 000 r.p.m.). The solid hydrolytic products were subsequently washed with doubly distilled water and then dried at 60°C for 24 h. Ageing of the precipitation systems was performed in glass autoclaves. The amorphous rhodium hydrous oxides obtained were subjected to thermal treatment in the temperature range 300–1000°C. The phase composition of the samples obtained after the thermal treatment of the amorphous precursors, as determined by X-ray powder diffraction (XRD), is given in Tables 2 and 3. X-ray powder diffraction measurements were performed at room temperature using a Phillips counter diffractometer (model MPD 1880, CuKα radiation, proportional counter, graphite monochromator). The crystallite size of the dominant phase in the samples was estimated using the Scherrer equation

Table 1
Experimental conditions for the preparation of the samples from 0.1 M $Rh(NO_3)_3$ solution at 90°C using NaOH or urotropin as a source of OH^- ions[a]

Sample	Urotropin (M)	Ageing time (days)	Starting pH adjusted with NaOH solution	Final pH
S2		1	9.00	7.61
S3		3	8.99	7.78
S4		7	9.01	7.11
S5		21	9.37	6.70
S6	0.25	1		6.97
S7	0.25	3		8.20
S8	0.25	7		9.18
S9	0.25	21		9.30
S10	0.25	90		9.42

[a] XRD patterns of samples S2–S10 showed that they were amorphous.

Table 2
Thermal treatment of amorphous rhodium hydrous oxide (sample S1) and the results of XRD phase analysis. Amorphous rhodium hydrous oxide was precipitated from an $Rh(NO_3)_3$ solution by adding a concentrated NH_3 aqueous solution of pH~10.4

Temp. of heating (°C)	XRD phase composition (approx. molar fraction)	Crystallite size[b] (nm)
60[a]	Amorphous	
160[a]	Amorphous	
400	Amorphous	
500	α-Rh_2O_3 (corundum type)	9 (2) (VBDL)
	RhO_2 (rutile type) (0.15)	
650	α-Rh_2O_3 (corundum type)	18 (3) (BDL)
900	α-Rh_2O_3 (corundum type)	
	β-Rh_2O_3 (0.50)	
900	β-Rh_2O_3	
(in argon)	Rh (0.05)	
1000	β-Rh_2O_3	

[a] Dried for 24 h.
[b] VBDL, very broad diffraction line; BDL, broad diffraction line.

$$D = \frac{0.9\lambda}{\beta_{1/2} \cdot \cos\theta}$$

where λ is the X-ray wavelength (CuKα), θ the Bragg angle and $\beta_{1/2}$ the full width of the diffraction line at half the maximum intensity.

The FT-IR spectra were recorded using a Perkin-Elmer spectrometer (model 2000). The program INFRARED DATA MANAGER (IRDM), also supplied by Perkin-Elmer, was used. A potassium bromide matrix was used.

The thermal behavior of selected samples was investigated at up to 900°C using an instrument produced by Netzsch. The temperature was controlled by a Pt–PtRh (10%) thermocouple, with a heating rate of 10°C per/min. In some DTA/TGA measurements argon was used as the purging gas.

3. Results and discussion

Amorphous rhodium hydrous oxide, precipitated from an $Rh(NO_3)_3$ solution with a concentrated NH_4OH solution at pH~10.4, was thermally treated at up to 1000°C. The results of the XRD phase analysis of the thermal decomposition products are given in Table 2, whereas the characteristic XRD patterns of selected samples are shown in Fig. 1. The samples produced by heating at up to 400°C were amorphous, in accordance with XRD measurements. After the calcination of the starting material at up to 500°C, two crystalline phases, α-Rh_2O_3 and RhO_2, appeared, thus indicating oxidation, $Rh^{3+} \rightarrow Rh^{4+}$. With a further increase in the heating temperature to 650°C in air, the RhO_2 decomposed (the reduction $Rh^{4+} \rightarrow Rh^{3+}$) and only α-$Rh_2O_3$ was detected by XRD. The average crystallite size of α-Rh_2O_3, estimated from XRD line broadening, increased from 9 to 18 nm with an increase in the temperature from 500 to 650°C. In the sample produced after calcination at 900°C in air, β-Rh_2O_3 additionally crystallized to α-Rh_2O_3. Under the reductive conditions at 900°C in argon, rhodium metal was formed as an associated phase of β-Rh_2O_3. A sample heated at 1000°C in air contained only β-Rh_2O_3. In order to obtain more data

Table 3
Thermal treatment of amorphous rhodium hydrous oxide and the results of XRD phase analysis. Amorphous rhodium hydrous oxide was prepared from an $Rh(NO_3)_3$ solution by adding an NaOH solution or urotropin as a source of OH^- ions

Sample	Heating temp. (°C)	XRD phase composition (approx. molar fraction)	Crystallite size of the dominant phase (nm)
S2	400	α-Rh_2O_3 + RhO_2 (0.3)	6 (2)
	500	α-Rh_2O_3	15 (4)
	600	α-Rh_2O_3	18 (4)
	900	α-Rh_2O_3 + β-Rh_2O_3 (0.1)	37 (8)
S3	400	Amorphous	
	500	α-Rh_2O_3 + RhO_2 (0.3)	6 (2)
	650	α-Rh_2O_3 + RhO_2 (0.03)	20 (5)
	900	α-Rh_2O_3 + β-Rh_2O_3 (0.05)	28 (7)
S4	400	Amorphous	
	500	α-Rh_2O_3 + RhO_2 (0.2)	10 (3)
	650	α-Rh_2O_3 + RhO_2 (0.1)	18 (4)
	900	α-Rh_2O_3 + β-Rh_2O_3 (0.03)	24 (6)
S5	400	Amorphous	
	500	α-Rh_2O_3 + RhO_2 (0.2)	7 (2)
	650	α-Rh_2O_3	13 (3)
	900	α-Rh_2O_3	20 (5)
S6	300	Rh + amorphous fraction	6 (2)
	600	β-Rh_2O_3 + Y[a]	40 (8)
	825	β-Rh_2O_3 + α-Rh_2O_3 (0.4)	28 (6)

[a] Y, unidentified phase.

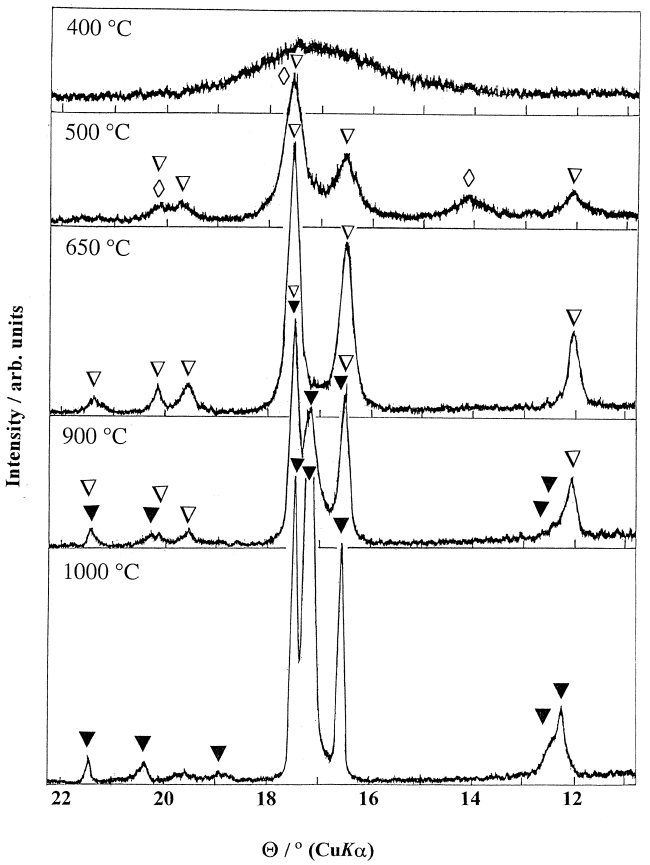

Fig. 1. Characteristic parts of powder XRD patterns (recorded at 25°C) of the samples obtained after the thermal treatment of sample S1 in the temperature range from 400 to 1000°C; △, α-Rh_2O_3; ▼, β-Rh_2O_3; ◊, RhO_2.

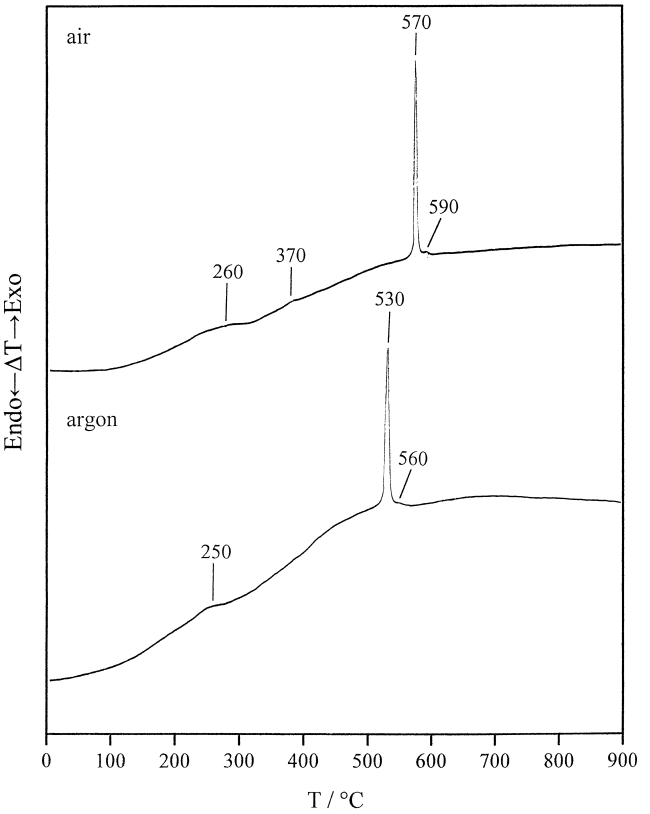

Fig. 2. DTA curves of sample S1 recorded in air or argon atmosphere.

about the thermal behavior of amorphous rhodium hydrous oxide, the starting material was subjected to differential thermal and thermogravimetric analysis, both in air and argon. DTA and TGA curves are shown in Figs. 2 and 3. The DTA curve recorded in air showed two very broad exothermic peaks of small intensity at 260 and 370°C. These peaks can be related to the incomplete crystal ordering of the oxide phases. A sharp and high intensity exothermic peak positioned at 570°C and a small intensity peak at 590°C can be attributed to the appearance of the well-crystallized oxide phases. In an argon atmosphere, these two peaks were shifted to lower temperatures, 530 and 560°C. The displacement of the peaks to lower temperatures when the measurement was carried out in argon indicated a difference in the chemistry of the thermal decomposition of the rhodium hydrous oxide precursor, depending on the oxidative or reductive atmospheres. Heating in an argon atmosphere leads to a partial autoreduction of the rhodium metal, as shown by XRD, and on the basis of this fact the accelerating effect of Rh° on the crystallization of rhodium oxides in argon can be suggested. Tomczak et al. [8] have investigated the influence of ambient atmosphere, temperature and proton

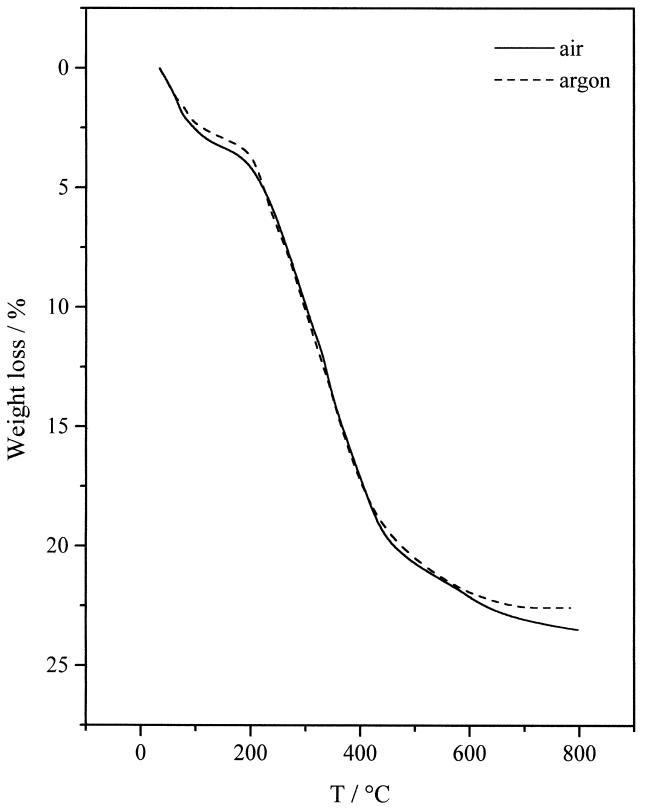

Fig. 3. TGA curves of sample S1 recorded in air or argon atmosphere.

concentration on the formation of rhodium species supported on a zeolite. Heating of the exchanged catalyst in the argon atmosphere at 500°C led to a 100% autoreduction in the rhodium metal and the formation of rather large rhodium particles, whereas calcination in an O_2 atmosphere at 380°C produced a mixture of the oxides RhO_2 and Rh_2O_3 and the 'free' ionic states of Rh^{3+} and Rh^{+}. After calcination at 500°C, Rh_2O_3 was the only oxide present. Musić et al. [9] have investigated the influence of the atmosphere during the thermal treatment of amorphous chromium hydroxide. The sharp exothermic peak between 410 and 420°C recorded in air could be related to the crystallization of Cr_2O_3. When the heating of amorphous chromium hydroxide was performed in argon, this exothermic peak shifted to 600°C. The accelerated crystallization of Cr_2O_3 from amorphous chromium hydroxide gel observed in air was explained by the catalytic effect of the higher oxidation states of the chromium species, which were probably restricted to the surface of the particles.

The TGA curves (Fig. 3) showed a TG loss of 20–25% of the initial mass during the heating of the sample in different atmospheres (air or argon) up to 800°C. The main TG loss was observed during heating at up to 600°C. The first abrupt weight loss observed in the TGA curve in air corresponds to the elimination of free water from amorphous sample. With a further increase of the temperature there is a second abrupt decrease of weight due to the elimination of structural water and incomplete crystal ordering of oxide phases with two inflection points in accordance with the exothermic peaks in the corresponding DTA curve. The inflection point close to 600°C is due to the ordering of well-crystallized oxide phases in accordance with DTA and XRD results.

Fig. 4 shows the FT-IR spectra of the samples produced by heating the amorphous rhodium hydrous oxide between 160 and 1000°C. Samples heated to 400°C showed a broad IR band centered at 544 cm^{-1}. Williams et al. [10] used SER (surface-enhanced-Raman) spectroscopy to monitor the surface properties of the rhodium catalyst during methanol oxidation. The presence of rhodium oxide (Rh_2O_3) was suggested on the basis of Raman bands, varying between 500 and 580 cm^{-1}, depending on the temperature. The heating of rhodium in oxygen at 350°C generated a Raman band at 530 cm^{-1} [11], which was usually attributed to the metal–oxygen stretch (ν_{Rh-O}) in Rh_2O_3. Kellogg [12] also investigated the formation of thin oxide layers and their reduction on a rhodium surface as a function of a wide range of oxidizing conditions. By means of imaging atom-probe analysis, it was found that stoichiometric Rh_2O_3 was formed at 133 Pa O_2 and temperatures of 500 K and above.

The FT-IR spectrum of the sample produced at 500°C showed the main features of α-Rh_2O_3. These spectral features were better pronounced for α-Rh_2O_3 produced as the single phase at 650°C. Three dominant IR bands at 655, 610 and 462 cm^{-1} were recorded. A pronounced

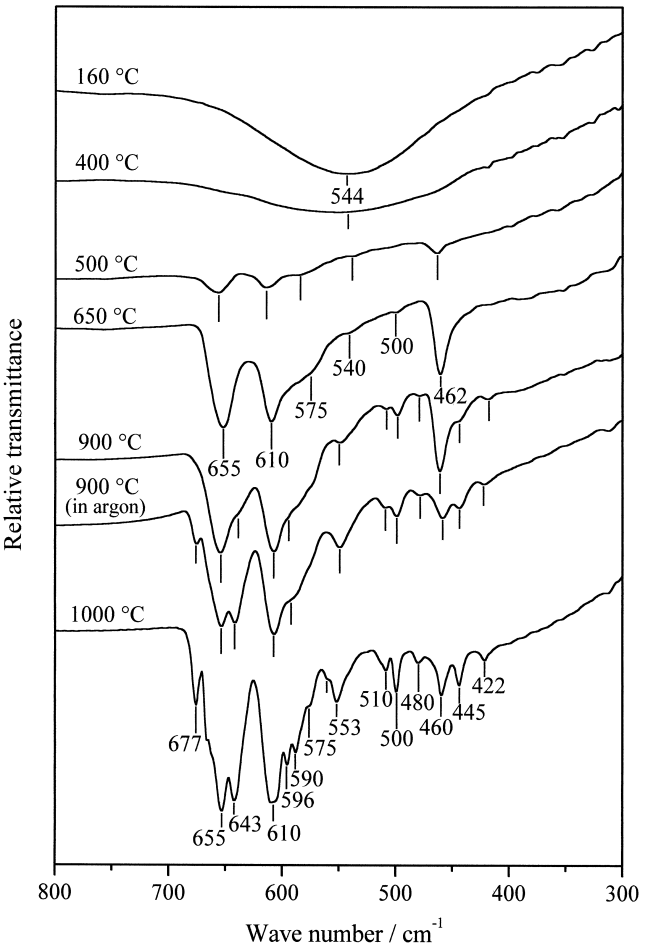

Fig. 4. FT-IR spectra of the samples obtained after the heating of sample S1 in the temperature range from 160 to 1000°C. The spectra were recorded at room temperature.

shoulder at 575 cm^{-1} and small intensity bands at 540 and 500 cm^{-1} were also visible. The recorded FT-IR spectrum of α-Rh_2O_3 can be related to the spectra of α-Fe_2O_3 and α-Cr_2O_3, as presented by Serna et al. [13]. Fig. 5 shows the FT-IR spectra of these corundum-type oxides, Cr_2O_3 (commercial, 99.999%, Ventron) and α-Fe_2O_3 (p.a. Merck), and of α-Rh_2O_3 prepared in the present work. The oxygen octahedra are more distorted for α-Rh_2O_3 than for α-Fe_2O_3 because Rh^{3+} is a larger cation than Fe^{3+} [14]. Each Rh^{3+} ion is surrounded by three oxygen neighbors at a distance of (2.03±0.03) Å and three oxygen neighbors at a distance of (2.07±0.04) Å. Within the oxygen octahedron, the distance between the oxygen ions in the same layer is either 2.62±0.09 or (3.14±0.05) Å, whereas the distance between adjacent oxygen ions in different layers is 2.78±0.02 or (2.94±0.02) Å. The separation of a *c* axis cation pair, r_c=(2.72±0.02) Å and of a 'basal plane' pair, r_a=(3.03±0.01) Å. The structural properties of α-Fe_2O_3 and Cr_2O_3 and the reflection of their structure on the spectroscopic or thermal behavior are discussed in the literature [15–18].

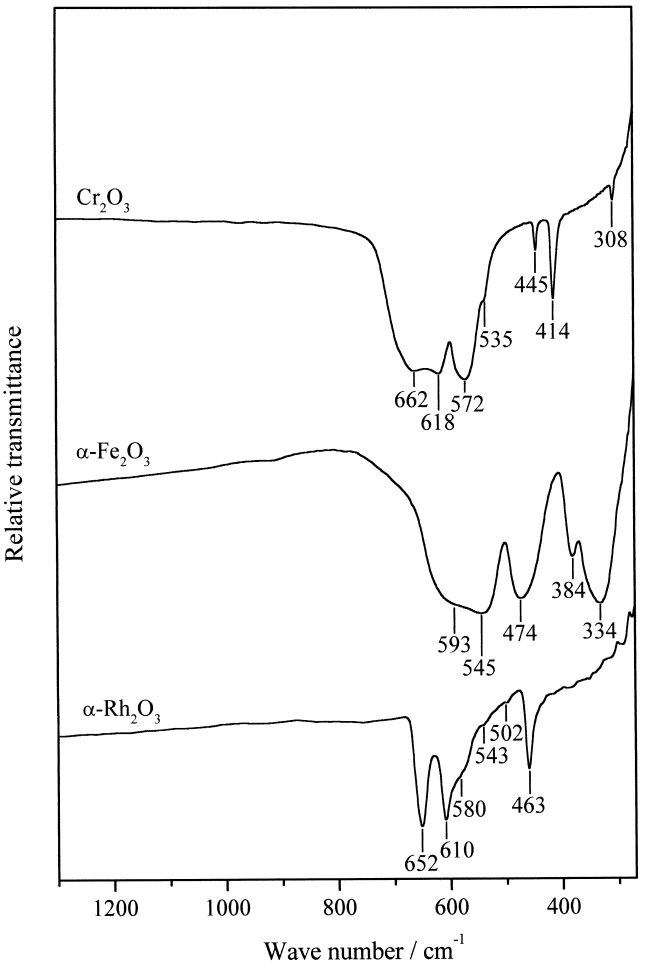

Fig. 5. FT-IR spectra of commercial Cr_2O_3 and α-Fe_2O_3, and of the α-Rh_2O_3 prepared in the present work. The spectra were recorded at room temperature.

The FT-IR spectrum of the sample produced at 1000°C can be related to the IR spectrum of β-Rh_2O_3, as previously published [19]. However, the FT-IR spectrum of the β-Rh_2O_3 synthesized in the present work contains more detail. During the thermal treatment of amorphous rhodium hydrous oxide, the formation of RhO_2 as the single or dominant phase was not observed. Schünemann et al. [20] exchanged NaY zeolite with Rh^{3+} ions and then reduced Rh^{3+} with H_2 to Rh°. After the oxidation of the thus reduced rhodium with O_2 at 1 bar, the formation of RhO_2 as the dominant phase at 320°C was observed, whereas Rh_2O_3 was the dominant phase after the oxidation of rhodium in zeolite at 500°C. Evidently the zeolite matrix played a certain role in the formation of the rhodium oxide phases with various oxidation states of rhodium. Besides the influence of the matrix, the particle size of the rhodium also has a significant influence on its redox properties [21].

Amorphous rhodium hydrous oxides, precipitated from 0.1 M $Rh(NO_3)_3$ solution by the addition of an NaOH solution at pH~9 (Table 1), were thermally treated at up to 900°C. Before the thermal treatment, the amorphous rhodium hydrous oxides were hydrothermally treated at 90°C for 1, 3, 7 and 21 days. After the ageing of the suspensions for a given time, the crystalline oxide phases were not observed, as shown by XRD. The results of the XRD phase analysis of the thermal decomposition products and approximate molar fractions are summarized in Table 3. Only in the sample hydrothermally treated for 1 day, after calcination at 400°C, were two crystalline phases observed, α-Rh_2O_3 and RhO_2. At higher temperatures the rutile-type oxide RhO_2 decomposed irreversibly to α-Rh_2O_3, which was present as the single phase at 500 and 600°C, according to the XRD phase analysis. In the sample produced after calcination at 900°C, β-Rh_2O_3 additionally crystallized to α-Rh_2O_3, which was the dominant phase. The crystallite size of α-Rh_2O_3 increased gradually from 6(2) to 37(8) nm, with an increase in the temperature from 400 to 900°C. The amorphous rhodium hydrous oxides obtained by hydrothermal treatment with longer ageing times (3, 7 and 21 days), after heating to 400°C were also amorphous in accordance with the XRD measurements.

In a sample aged for 3 days at 90°C, after its calcination at 500°C, a mixture of two crystalline phases, α-Rh_2O_3 and RhO_2 was found. The approximate molar fraction of RhO_2, which was present as the minor phase, decreased about ten times with the increase in the temperature from 500 to 650°C. With a further increase in the heating temperature to 900°C, the small fraction of RhO_2 was reduced to Rh_2O_3. A small fraction of β-Rh_2O_3 in the sample produced at 900°C was also observed. The temperature treatment caused an increase in the crystallite size of α-Rh_2O_3 from 6(2) to 28(7) nm in the temperature range 500–900°C. A similar tendency in the progress of crystallization during the thermal treatment of amorphous rhodium hydrous oxide, obtained after 7 days of ageing at 90°C, was observed for applied temperatures. However, during the thermal treatment of amorphous rhodium hydrous oxide, which was obtained by ageing treatment for 21 days at 90°C, the route of crystallization was changed in comparison to those described above. The sample produced by heating amorphous rhodium hydrous oxide to 400°C was also of an amorphous nature. After heating to 500°C, two crystalline phases, α-Rh_2O_3 and RhO_2, appeared, and after heating to 650°C the rutile-type oxide, RhO_2, which was present as the minor phase in previous samples, irreversibly decomposed to α-Rh_2O_3, as determined by XRD. With a further increase in the heating temperature to 900°C, α-Rh_2O_3 was present as the single phase. Wold et al. [22] reported the existence of two structural forms of Rh_2O_3, a hexagonal low-temperature form with a corundum structure, which transformed into a high-temperature orthorhombic form upon heating above 750°C. The hexagonal low-temperature form was prepared by precipitating the hydrated rhodium oxide and heating it in air at 700°C. A high-temperature orthorhombic form could be obtained by the above-mentioned irreversible transformation over the temperature range 750–1000°C or

converted directly by the oxidation of finely dispersed rhodium at 1000°C.

Our experiments undoubtedly indicated the strong influence of the nature of amorphous rhodium hydrous oxide on its thermal behavior. Despite the fact that all the starting rhodium hydrous oxides aged between 1 and 21 days were amorphous, the phase composition of their thermal decomposition products varied depending on the ageing time. In the present case, amorphous rhodium hydrous oxide (amorphous $Rh(OH)_3$) was precipitated by the abrupt addition of an NaOH solution. It is realistic to suppose that with the heating of this precursor at 90°C, the process of the nucleation and crystallization of rhodium oxide or the oxyhydroxide phase was started. With prolonged ageing, this crystallization process advanced. After the heating of amorphous rhodium hydrous oxides at 400 and 500°C, the α-Rh_2O_3 crystallites were of very small size (Table 3). The crystallite size of α-Rh_2O_3 crystallites obtained up to 400°C was 6 nm, whereas with the increase of the temperature to 500°C the corresponding crystallite size increased to 15 nm, for example, in sample S2. One day of ageing the amorphous precursor at 90°C probably produced only a very short range ordering, as manifested by very faint modulations of an amorphous XRD pattern. It can be concluded that this precursor remained (almost) amorphous, which on additional heating at 400°C crystallized to a mixture of α-Rh_2O_3 and RhO_2. With prolonged ageing at 90°C, between 3 and 21 days, the crystallization process advanced sufficiently to increase the temperature of the appearance of the crystalline oxide phases following the thermal treatment of these precipitates. It can be concluded on the basis of these experiments that during the ageing of the suspension of amorphous rhodium hydrous oxide at 90°C, only a very short-range ordering took place, which was the basis for the nucleation of very small crystallites. Therefore, one might conclude that the onset of the crystallization process occurred in the suspension of amorphous rhodium hydrous oxide aged at 90°C. Amorphous rhodium hydrous oxides aged for 21 days at 90°C yielded α-Rh_2O_3 as the single phase at 650 and 900°C.

The results of differential thermal and thermogravimetric analysis are shown in Figs. 6 and 7. Although all the precursors obtained for different ageing times were amorphous, the DTA curves recorded in air indicated that their thermal behavior depended on the ageing time. The exothermic peak positioned at 575°C, observed for the amorphous precursor aged for 1 day at 90°C, can be attributed to the transformation of this precursor to crystalline α-Rh_2O_3. For other amorphous precursors, aged between 3 and 21 days at 90°C, this exothermic peak was shifted to 610°C. A gradual shift of the peak at 575°C to higher temperatures with prolonged ageing of the amorphous precursor can be also used as a sign of the progress of the crystallization process, in accordance with the XRD analysis of the thermal decomposition products. The DTA

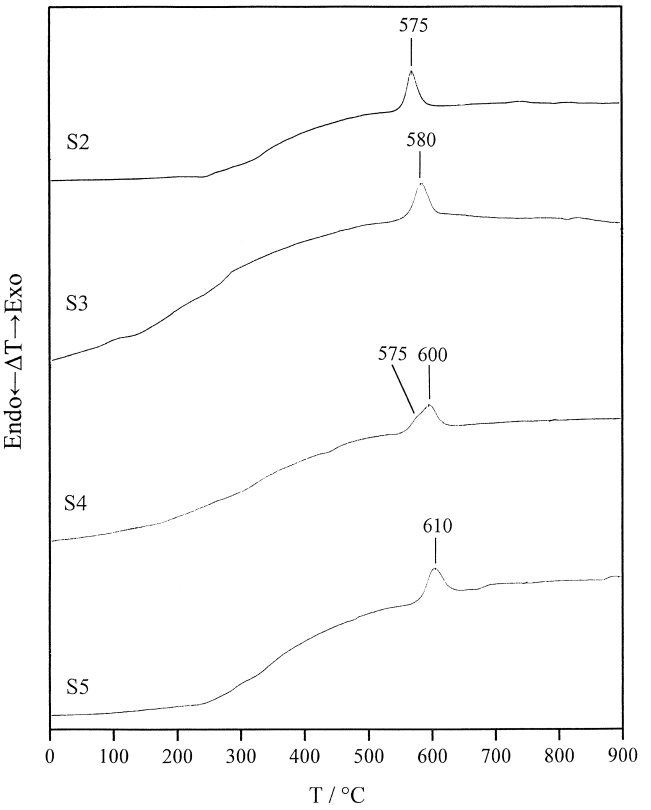

Fig. 6. DTA curves of samples S2–S5, recorded in air.

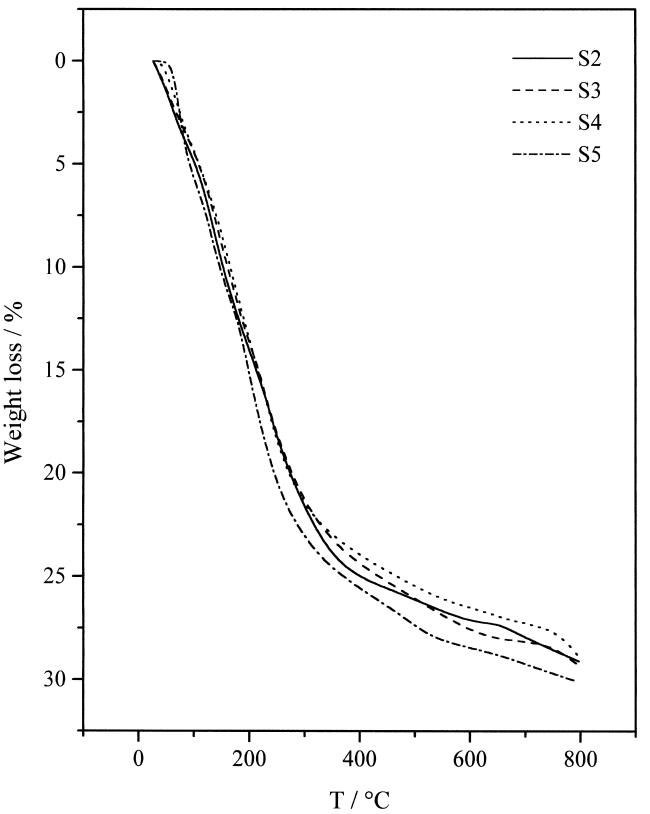

Fig. 7. TGA curves of samples S2–S5, recorded in air.

curve obtained for the precursor aged for 7 days at 90°C showed the superposition of two exothermic peaks at 575 and 600°C, due to two different oxide phases. The TGA curves (Fig. 7) showed a loss of ~30% of the initial mass during the heating of the sample to 800°C.

The thermal behavior of amorphous rhodium hydrous oxides aged for different times at 90°C was also monitored with FT-IR spectroscopy and the corresponding results are summarized in Figs. 8 and 9. Fig. 8 shows the FT-IR spectra of the samples produced by heating the series of amorphous precursors at 400°C, characterized by various ageing times at 90°C. The FT-IR spectrum of the precursor aged for 1 day after heating at 400°C showed the main features of α-Rh_2O_3, in contrast to the FT-IR spectra of the precursors aged for longer times, which exhibited a completely amorphous character. The spectral features of α-Rh_2O_3 were more and more pronounced as the temperature increased to 650°C (Fig. 9). α-Rh_2O_3 was monitored on the basis of dominant IR bands at 655, 610 and 462 cm^{-1}, small intensity bands at 541, 500 and 420 cm^{-1} and a shoulder at 580 cm^{-1}.

In the present work, amorphous rhodium hydrous oxides were also precipitated from an $Rh(NO_3)_3$ solution in the presence of urotropin at 90°C. In acidic pH medium at elevated temperatures, urotropin undergoes chemical decomposition in accordance with the following formal chemical reactions

$$(CH_2)_6N_4 + 6H_2O \rightarrow 4NH_3 + 6HCHO \quad (1)$$

and

$$NH_3 + H_2O \rightarrow NH_4^+ + OH^- \quad (2)$$

and thus serves as a generator of OH^- ions [23]. Amorphous precipitates prepared in the presence of decomposing urotropin were subjected to thermal treatment. However, during the thermal treatment of these precipitates, explosion effects were observed. These effects are dependent on the heating rate. In the case of very small heating rates, this can be avoided. These explosion effects had an impact on the phase composition of the reaction products. Amorphous rhodium hydrous oxide precipitated for 1 day in the presence of urotropin at 90°C was additionally heated in a quartz ampoule at 300°C in contact with air, which resulted in the production of rhodium metal, as determined by XRD. The crystallite size of the thus produced rhodium was 6(2) nm. With a further increase in the temperature to 600°C, a mixture of β-Rh_2O_3 and an unidentified phase (denoted by Y) were obtained, whereas after additional thermal treatment at 825°C, a mixture of β-Rh_2O_3 and α-Rh_2O_3 was found.

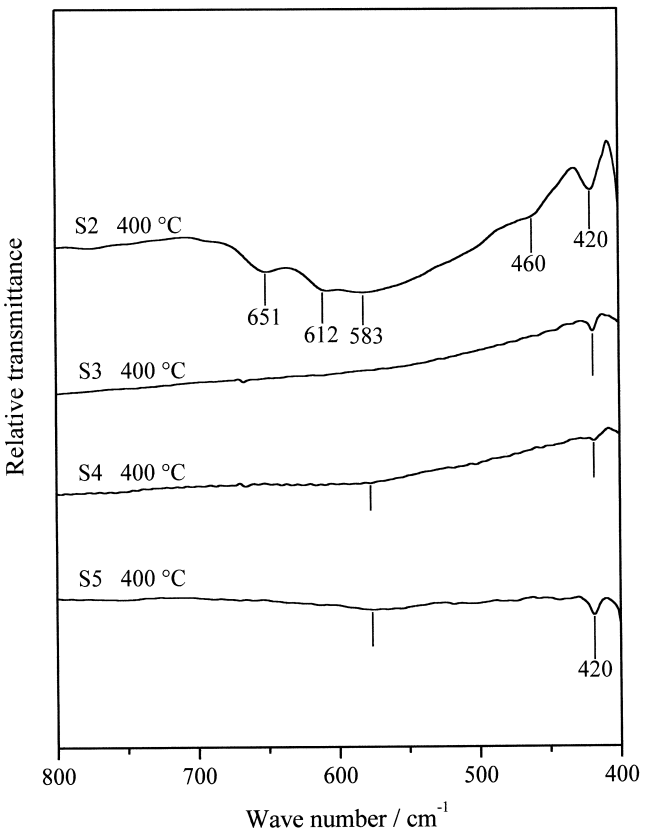

Fig. 8. FT-IR spectra of thermal decomposition products obtained after heating samples S2–S5 at 400°C. The spectra were recorded at room temperature.

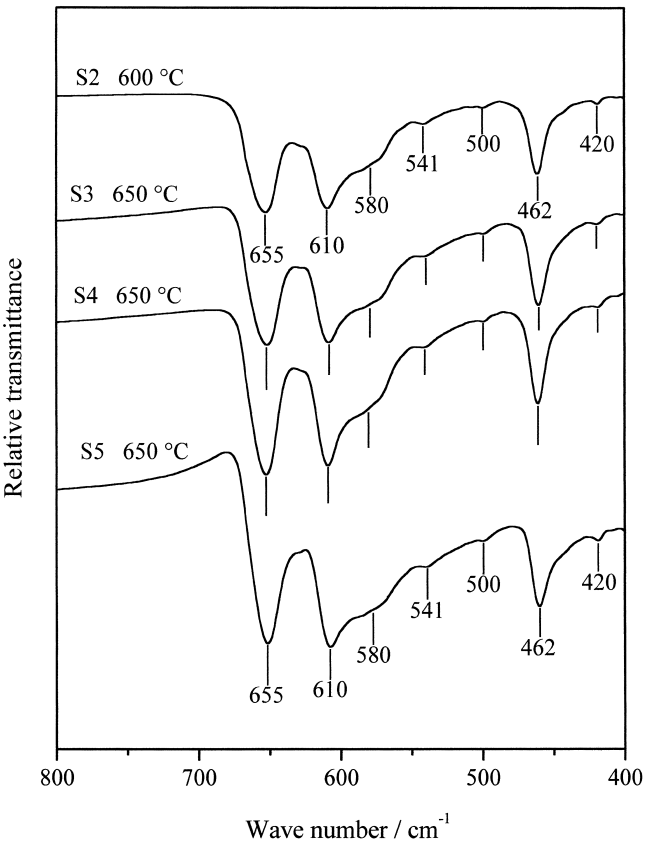

Fig. 9. FT-IR spectra of the thermal decomposition products obtained after the heating of samples S2–S5 at up to 650°C. The spectra were recorded at room temperature.

Fig. 10 shows the TGA curve recorded for sample S6 in air. An abrupt decrease in weight was detected and the greatest loss of 18.9% of the initial mass was observed at 270°C. With a further increase in the temperature, an increase in weight was visible due to the oxidation of nanocrystalline rhodium particles. The general behavior of the TGA curves observed for samples S7–S10 was in accordance with that observed for the TGA curve of sample S6.

These experiments, in addition to previous experiments, also demonstrated the strong influence of the precipitation chemistry on the thermal behavior of amorphous rhodium hydrous oxide. The formation of nanocrystalline rhodium powder is a very complex process. Traces of urotropin and nitrate anions which were not washed out from the precipitate are sufficient to start explosive reactions. The same is valid for HCHO and its chemical condensation products in a mixture with nitrates. On the other hand, rhodium ions by themselves are a very effective catalyst for the reaction of denitration [24]. In these reactions, the chemical decomposition of OH^- ions is probably also included and the final result of all these reactions is the reduction of Rh^{3+} to Rh°. The formation of nanocrystalline rhodium was reproducible and the crystallite size varied in the range of the error typical for the Scherrer method. To the best of our knowledge, the reduction of amorphous rhodium hydrous oxide to Rh° in air at a moderate temperature has not been previously published. These reactions can be explored for the preparation of nanocrystalline rhodium for catalytic applications.

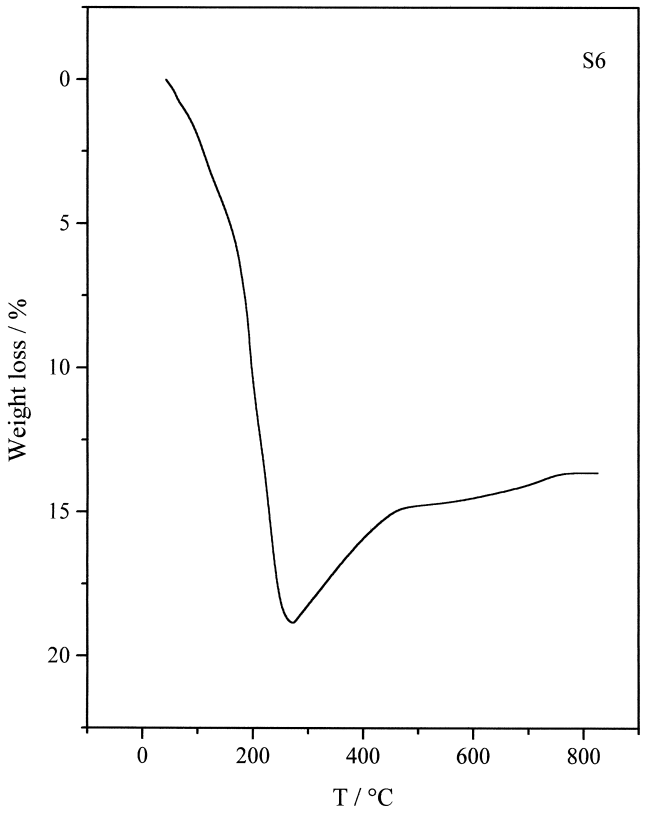

Fig. 10. TGA curve of sample S6, recorded in air.

References

[1] G. Bayer, H.G. Wiedemann, Thermochim. Acta 15 (1976) 213.
[2] E. Moran-Miguelez, M.A. Alario-Franco, Thermochim. Acta 60 (1983) 181.
[3] I.I. Prosychev, V.B. Lazarev, I.S. Shaplygin, Zh. Neorg. Khim. 22 (1977) 2078.
[4] S.J. Crimp, L. Spiccia, Aust. J. Chem. 48 (1995) 557.
[5] Yu.E. Roginskaya, O.V. Morozova, G.I. Kaplan, R.R. Shifrina, M. Smirnov, S. Trasatti, Electrochim. Acta 38 (1993) 2435.
[6] S. Gottesfeld, J. Electrochem. Soc. 127 (1980) 272.
[7] G. Jerkiewicz, J.J. Borodzinski, J. Chem. Soc. Faraday Trans. 90 (1994) 3669.
[8] D.C. Tomczak, G.D. Lei, V. Schünemann, H. Trevino, W.M.H. Sachtler, Microporous Mater. 5 (1996) 263.
[9] S. Musić, M. Maljković, S. Popović, R. Trojko, Croat. Chem. Acta 72 (1999) 789.
[10] C.T. Williams, C.G. Takoudis, M.J. Weaver, J. Phys. Chem. B 102 (1998) 406.
[11] C.T. Williams, E.K.-Y. Chen, C.G. Takoudis, M.J. Weaver, J. Phys. Chem. B 102 (1998) 4785.
[12] G.L. Kellogg, Surf. Sci. 171 (1986) 359.
[13] C.J. Serna, J.L. Rendon, J.E. Iglesias, Spectrochim. Acta 38A (1982) 797.
[14] J.M.D. Coey, Acta Cryst. B26 (1970) 1876.
[15] C.M. Flynn Jr., Chem. Rev. 84 (1984) 31.
[16] I.D. Brown, R.D. Shannon, Acta Cryst. A29 (1973) 266.
[17] P. Ratnasamy, A.J. Léonard, J. Phys. Chem. 76 (1972) 1838.
[18] H. Sawada, Mater. Res. Bull. 29 (1994) 239.
[19] K.R. Poeppelmeier, J.M. Newsam, J.M. Brown, J. Solid State Chem. 60 (1985) 68.
[20] V. Schünemann, B. Adelman, W.M.H. Sachtler, Catal. Lett. 27 (1994) 259.
[21] D. Martin, D. Duprez, Appl. Catal. A: General 131 (1995) 297.
[22] A. Wold, R.J. Arnott, W. J Croft, Inorg. Chem. 2 (1963) 972.
[23] A. Šarić, S. Musić, K. Nomura, S. Popović, Croat. Chem. Acta 71 (1998) 1019.
[24] S. Musić, M. Ristić, S. Popović, J. Radioanal. Nucl. Chem. 134 (1989) 353.